Probing the magnetic structure of a pair of transpolar arcs with a solar wind pressure step

Stephen, E. Milan[1], Jennifer, Alyson Carter[1], and Benoit Hubert[2]

[1]University of Leicester
[2]University of Liege

November 21, 2022

Abstract

We present observations of the northern hemisphere auroras taken with the Far UV cameras onboard the Imager for Magnetopause-to-Aurora Global Exploration (IMAGE) spacecraft during a compression of the magnetosphere by a solar wind pressure step on 30 December 2001. The compression occurs during a period of northward IMF which has given rise to the presence of a pair of transpolar arcs (TPAs) near the dawnside oval. The compression causes a brightening of the oval, from dayside to nightside over the course of 10 mins, followed by a brightening of the midnight sector oval and TPAs from nightside to dayside, again over 10 mins. We suggest that the brightening is caused by pitch angle scattering of particles trapped on closed magnetic field lines, and that the sequence of the brightening tracks the solar wind pressure step as it progresses along the length of the magnetotail. Travelling at 600 km s$ˆ{-1}$, the step reaches up to 90 R_E down-tail over the period of brightening, suggesting that the magnetic field lines which map to the TPAs are closed and stretch almost this length down-tail.

Probing the magnetic structure of a pair of transpolar arcs with a solar wind pressure step

S. E. Milan[1*], J. A. Carter[1], and B. Hubert[2]

[1]Department of Physics and Astronomy, University of Leicester, Leicester, UK.
[2]Laboratory for Planetary and Atmospheric Physics, University of Liège, Liège, Belgium.

Key Points:

- A solar wind pressure step causes a brightening of the auroral oval and a pair of transpolar arcs (TPAs)
- The oval brightens from dayside to nightside, and then the TPAs brighten from nightside to dayside
- The TPAs comprise closed field lines which stretch up to 90 R_E down-tail

*Department of Physics and Astronomy, University of Leicester, Leicester LE1 7RH, UK

Corresponding author: Steve Milan, `steve.milan@le.ac.uk`

Abstract

We present observations of the northern hemisphere auroras taken with the Far UV cameras onboard the Imager for Magnetopause-to-Aurora Global Exploration (IMAGE) spacecraft during a compression of the magnetosphere by a solar wind pressure step on 30 December 2001. The compression occurs during a period of northward IMF which has given rise to the presence of a pair of transpolar arcs (TPAs) near the dawnside oval. The compression causes a brightening of the oval, from dayside to nightside over the course of 10 mins, followed by a brightening of the midnight sector oval and TPAs from nightside to dayside, again over 10 mins. We suggest that the brightening is caused by pitch angle scattering of particles trapped on closed magnetic field lines, and that the sequence of the brightening tracks the solar wind pressure step as it progresses along the length of the magnetotail. Travelling at 600 km s^{-1}, the step reaches up to 90 R_E down-tail over the period of brightening, suggesting that the magnetic field lines which map to the TPAs are closed and stretch almost this length down-tail.

Plain Language Summary

The auroras usually take the form of ovals surrounding the geomagnetic poles, but occasionally an auroral feature bisects the dim region within the ovals: a transpolar arc. Although the geomagnetic conditions that give rise to TPAs are well-understood, there is continued controversy regarding how TPAs are formed and the structure of the magnetosphere during their presence: are the magnetic field lines associated with the TPA connected into the interplanetary medium outside the magnetosphere (are open), or do they link from one hemisphere to the other (are closed). In this study we use observations of the brightening of the auroral oval and a pair of TPAs in response to a sharp increase in the pressure of the solar wind. The oval first brightens from the dayside to the nightside, and then the TPAs brighten from nightside to dayside, allowing us to track the progression of the solar wind step along the length of the magnetotail. This confirms that the TPA field lines are closed and stretch for up to 90 Earth radii down-tail. This allows for the first time the magnetic structure of a TPA to be deduced, probing a region of the distant magnetotail that is rarely accessed by spacecraft.

1 Introduction

Auroral activity near the poles during periods of low geomagnetic activity was first reported in the 1910s and 1920s, and has been studied extensively ever since (see reviews by Zhu et al. (1997), Newell et al. (2009), Kullen (2012), Fear (2019), and Hosokawa et al. (2019)). Transpolar arcs (TPAs), sun-aligned arcs, and polar cap arcs, as such auroral features have variously been known, appear as auroral features that extend from the nightside auroral oval towards the dayside cusp, bisecting the otherwise dim polar cap region. They occur predominantly during periods of northward interplanetary magnetic field (IMF $B_Z > 0$), they typically form adjacent to the dawn or dusk sides of the auroral oval depending on the sense of IMF B_Y, and their subsequent motion dawnward or duskward is controlled by changes in the sense of IMF B_Y. Although this behaviour is now well-established, there remain many unanswered questions regarding the magnetospheric structure associated with TPAs, and the source of the plasma that precipitates to generate the auroral emission.

The main controversy is whether the magnetic field lines associated with the TPA are open (interconnected with the IMF) or closed (connected to the opposite hemisphere). The surrounding polar cap is open, magnetically conjugate with the magnetotail lobes. An early assumption was that TPAs were associated with flow shears in the polar cap convection pattern driven by lobe reconnection, leading to field-aligned currents carried by precipitating electrons (see, e.g., Carlson and Cowley (2005)). This does not straightforwardly explain the source of these electrons, as the magnetotail lobes are known to be generally devoid of plasma. Also, a shear flow can weaken and reform in another location, whereas TPAs appear to move from one location to another as coherent features. There are, however, high altitude plasma observations which suggest that regions of dense plasma can exist in the lobes, injected by lobe reconnection, giving rise to TPAs (Shi et al., 2013; Mailyan et al., 2015).

On the other hand, if TPA field lines are closed, what is the mechanism that gives rise to these closed flux regions embedded within the otherwise open lobes? Milan et al. (2005) proposed an extension of the expanding/contracting polar cap (ECPC) model (Cowley & Lockwood, 1992; Milan et al., 2003, 2007) that invoked magnetic reconnection in a twisted magnetotail to produce just such a closed field line region which protrudes into the polar cap. Apart from their unusual mapping into the ionosphere, such closed field regions would be similar to the normal plasma sheet, explaining the source of precipitating particles. Subsequent motion of the TPA was proposed to be controlled by lobe reconnection "stirring" the surrounding open flux of the polar cap. The model of Milan et al. (2005) made specific predictions about the dawn or dusk location of the formation of TPAs, dependent on IMF B_Y, and the conditions under which they would move. These predictions have largely been borne out by subsequent studies (e.g., Goudarzi et al. (2008); Fear and Milan (2012a, 2012b); Kullen et al. (2015); Carter et al. (2017); Reidy et al. (2018)). In addition, in situ measurements at high altitude above a TPA near the centre of the polar cap have shown a plasma sheet-like particle population with a double loss-cone, suggestive of closed field lines embedded within the otherwise open lobe (Fear et al., 2014). On the other hand, low altitude particle measurements have suggested that a TPA lying adjacent to the dusk or dawn auroral oval may not be separate from the plasma sheet, but just represent a poleward extension of the plasma sheet in that local time sector (Newell et al., 2009).

If TPAs are indeed closed, this suggests that they should form conjugate auroral phenomena in the two hemispheres, though the model of Milan et al. (2005) suggests that a duskside TPA in one hemisphere should map to a dawnside TPA in the other, at least initially after formation, before subsequent dawn-dusk motions take place. Simultaneous auroral imaging of both hemispheres is rare. However, conjugate TPAs have been observed (e.g., Carter et al. (2017); Reidy et al. (2018)), but there are also counterexamples in which a TPA is observed only in one hemisphere (e.g., Østgaard et al. (2003)).

This open/closed question may persist in part because it has been suggested that some polar cap arcs may form on open field lines and some on closed (e.g., Carlson and Cowley (2005); Newell et al. (2009); Reidy et al. (2018)). It seems likely, if this is the case, that the former would be weak sun-aligned arcs and the latter more large-scale, brighter TPA. However, the controversy remains: are some TPA closed? This also raises the question that, if TPAs are indeed closed, how do the field lines from one hemisphere map to the other, and specifically how far down-tail do these closed field lines stretch? This is difficult to answer as there is a dearth of in situ observations far down-tail, especially out of the equatorial plane where these closed field lines should be embedded within the open magnetotail lobes.

The present study goes some way to answering this question, by considering auroral observations from a period when the magnetosphere is struck by a solar wind pressure step, which causes a brightening of the auroral oval and a pair of pre-existing TPAs. The observed sequence of brightening suggests that the TPAs are indeed closed, and that these closed field lines stretch as far as 90 R_E behind the Earth.

2 Observations

Observations of the northern hemisphere auroras on 30 December 2001 are provided by the Far UV instrument onboard the Imager for Magnetopause-to-Aurora Global Exploration (IMAGE) spacecraft (Mende, Heetderks, Frey, Lampton, et al., 2000; Mende et al., 2000; Mende, Heetderks, Frey, Stock, et al., 2000). The Wideband Imaging Camera (WIC) and Spectrographic Imager (SI12) generated 10 s- and 5 s-integrated images of emissions produced by (predominantly) electron and proton precipitation, respectively, with a cadence of approximately 123 s. IMAGE was in an elliptical polar orbit that allowed imaging of the auroras for 10 h of each 14-h orbit. We also employ 1 min-cadence measurements of the IMF and solar wind by the Advanced Composition Explorer (ACE) spacecraft, and geomagnetic indices, accessed through the NASA OMNIWeb portal (King & Papitashvili, 2005). Observations of the northern hemisphere convection pattern from the Super Dual Auroral Radar Network (SuperDARN) (Chisham et al., 2007) are also reported, but not shown.

Figure 1 presents observations from 18 to 23 UT. Panels (a) to (d) show keograms derived from the WIC and SI12 images along the 12-00 (noon-midnight) and 18-06 (dusk-dawn) magnetic local time (MLT) meridians, down to 50° geomagnetic latitude. Auroral emission from the dayside portion of the WIC noon-midnight meridian below 70° latitude is obscured by dayglow; the SI12 observations are less affected by dayglow. Below this are presented in panel (e) the B_Y (blue) and B_Z (red) components of the IMF, (f) the solar wind speed, V_{SW}, and (g) the proton number density, N_{SW}. The bottom two panels show (h) the AU, AL, and (i) SYM-H geomagnetic indices.

The feature of most interest in this study is the step in solar wind ram pressure near 20:15 UT, seen here as sudden increases in V_{SW} from 450 to 600 km s^{-1} and N_{SW} from 5 to 15 cm^{-1}, corresponding to a change in pressure from 2 to 10 nPa, which produced a brightening of the auroras and a positive excursion of SYM-H. The solar wind data are time-shifted in the OMNI pre-processing to account for the propagation delay from ACE to the bow shock; clearly, the propagation time has been overestimated in the present case, and the pressure step actually impacted the magnetosphere at 20:09 UT (vertical green line).

Before describing this feature in more detail, we give some context to the interval as a whole. The IMF turned northward, with $B_Z \approx 15$ nT, at 06 UT (12 h before the start of Fig. 1); B_Y swung from +15 to -20 nT between 06 and 11 UT. By 18 UT, a TPA had formed adjacent to the dawn-sector auroral oval; the TPA emission can be clearly seen in the WIC observations in panel (b), adjacent to the dawn-side oval between 19:00 and 21:20 UT, including the time of the arrival of the pressure step. This emission is also present in the SI12 keogram, panel (d), but much less clearly. Occasionally during this period the TPA emission encroached on the noon-midnight meridian, at which times it is visible in panels (a) and (c), e.g., 19:20 to 20:20 UT and 21:20 to 22:10 UT.

Figure 2 shows the evolution of the WIC auroral morphology shortly before and after the arrival of the pressure step. The pre-existing TPA discussed above (which we label TPA1) is highlighted in panel (a). At this time, 18:53 UT, a second TPA (TPA2) was in the process of formation. As described by Milan et al. (2005), a brightening of the nightside oval is accompanied by an auroral feature that grows into the polar cap from one end, as seen at 19:13 UT, panel (b). This is accompanied by nightside ionospheric flows observed by SuperDARN (not shown) which are consistent with TRINNI activity (tail reconnection during IMF northward non-substorm intervals), as also predicted by Milan et al. (2005). By 20:07 UT, panel (c), just prior to the step arrival, the two TPAs lie adjacent and approximately parallel to each other.

As seen in Fig. 1, the location of the TPAs was unaffected by the arrival of the pressure step, as the IMF did not change orientation significantly at that time. Between 21:00 and 21:30 UT the IMF turned to $B_Z < 0$ and B_Y changed sign twice. The southward turning marked the onset of low latitude magnetopause reconnection, causing the polar cap to expand and the auroral oval to progress toward lower latitudes, accompanied by enhancements in AU and AL. The onset of dayside reconnection and the changes in

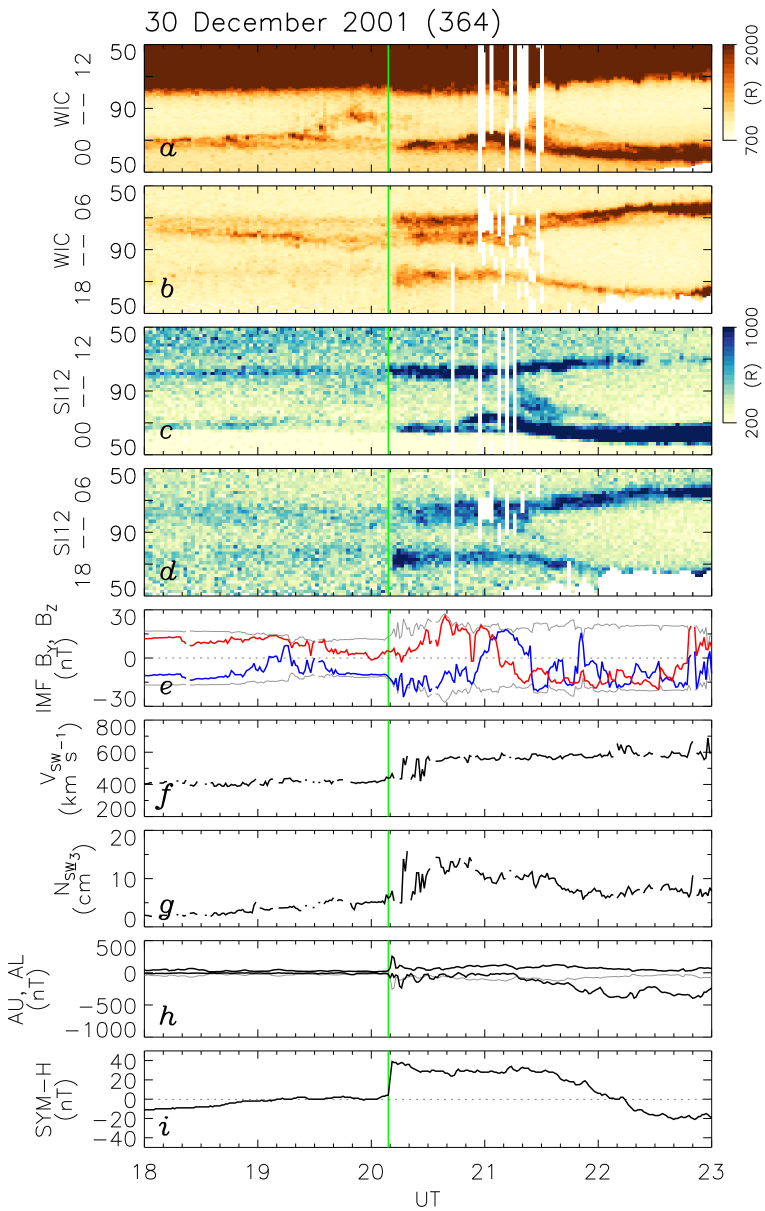

Figure 1. Observations of the northern hemisphere auroras and associated solar wind conditions and geomagnetic indices on 30 December 2001. Keograms of WIC observations along the (a) noon-midnight and (b) dawn-dusk meridians for geomagnetic latitudes above 50°; vertical white stripes indicate missing data. (c) and (d) Corresponding keograms from SI12 observations. (e) IMF B_Z (red) and B_Y (blue), (f) solar wind speed, and (g) solar wind density measurements from ACE; (h) AU and AL and (i) SYM-H geomagnetic indices. The arrival of a solar wind pressure step is indicated by a vertical green line at 20:09 UT.

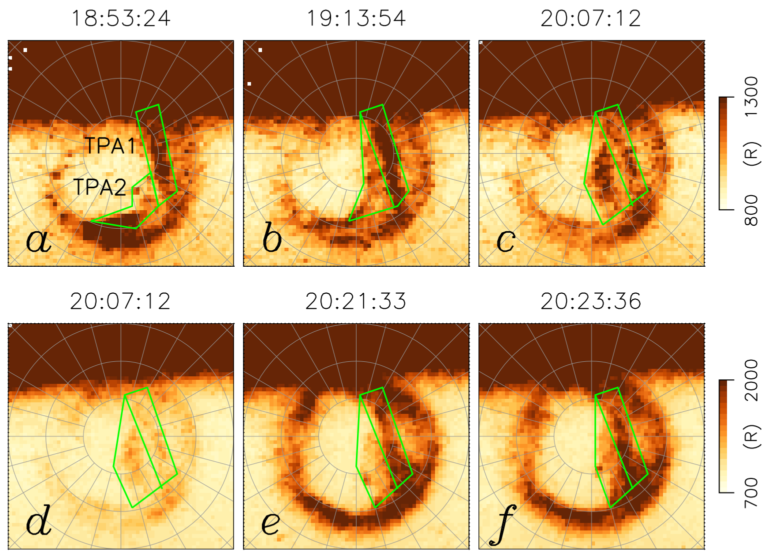

Figure 2. IMAGE WIC observations showing the evolution of the auroral morphology before and after the arrival of the pressure step. (a) A pre-existing transpolar arc (TPA1) is joined by the formation of a second (TPA2). Green boxes delineate TPA1 and TPA2. (b) TPA2 evolves to lie adjacent to TPA1. (c) The auroral morphology just prior to the step arrival, 20:07 UT. (d) Same as (c) but on the same colour scale as Figs. 1 and 3, which allows the auroral brightening to be studied. (e) and (f) Later stages in the brightening of TPA1 and then TPA2.

B_Y resulted in the TPAs moving duskward and antisunward, before merging with the nightside auroral oval.

We now investigate the brightening in response to the pressure step in more detail. Returning to Fig. 2, panel (d) shows the same image as panel (c), just before the arrival of the pressure step, but on a modified colour scale that allows the auroral brightening to be studied. By panel (e) at 20:21 UT the whole oval has brightened, as has TPA1, but TPA2 remains close to its original intensity. By panel (f), 20:23 UT, TPA2 has begun to brighten also.

Meurant et al. (2004) and Tsurutani et al. (2011) present sequences of auroral images that show that the auroral oval can brighten progressively in response to a solar wind pressure shock: first at noon, then around to earlier and later MLT meridians, and finally to the nightside (see also Zhou and Tsurutani (1999), Tsurutani et al. (2001), and Meurant et al. (2003)). This has been ascribed to the progression of the compressive effect of the pressure step around the flanks of the magnetosphere and along the magnetotail. Moreover, Meurant et al. (2004), using the SI12 and WIC cameras onboard IMAGE, demonstrated a dawn-dusk asymmetry in the auroral response to a shock, with electron auroras dominating at dawn and proton auroras at dusk. We might expect a similar response in the present set of observations, but we are also interested in how the TPAs respond. We note that examination of Fig. 1(b) suggests that although the auroral oval brightens promptly, the brightening of the TPAs is delayed by 10 or more minutes.

To examine this delay in more detail, Figure 3 presents the sequence of WIC and SI12 images (first and third rows, respectively) from just after the arrival of the step to 24 mins after. To aid the eye, the second and fourth rows present difference images, that

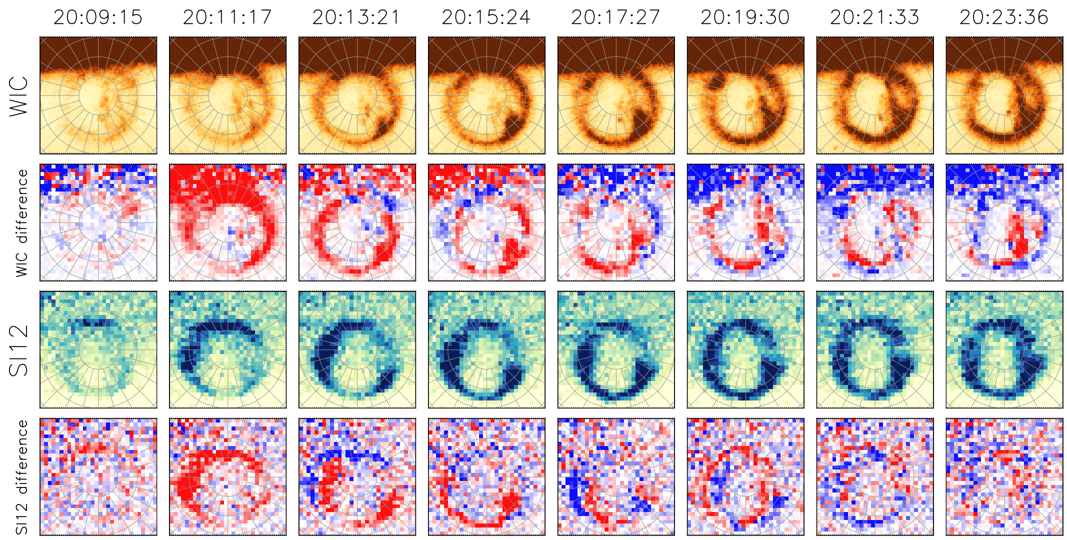

Figure 3. A sequence of IMAGE auroral observations from just after the arrival at the magnetopause of the solar wind pressure step on 30 December 2001. Magnetic latitudes of 80°, 70°, and 60° are shown by grey circles, and 12 MLT is at the top of each panel. The WIC and SI12 colour scales are the same as Fig. 1.

is, each image subtracted from the image immediately before, with red and blue indicating that the image has brightened or dimmed, respectively.

The first sign of the effect of the shock is a brightening of the dayside oval observed by SI12 at 20:09 UT. A similar effect is not seen by WIC at this time as dayglow encroaches on the dayside oval. By 20:11 UT the dayside and duskside of the oval has brightened in the SI12 observations, whereas in the WIC observations it is the dayside and dawnside that has brightened most significantly. This suggests that the increase in proton and electron precipitation is most significant at dusk and dawn, respectively, in agreement with Meurant et al. (2004). By 20:15 UT, the brightening has reached the midnight sector of the oval, in both SI12 and WIC images. Up until this point, the TPAs have remained largely unaffected. At 20:15 UT the nightside end of TPA1 begins to brighten. In subsequent images until 20:23 UT, two effects are observed, most clearly in the WIC difference images: firstly, in the midnight sector a brightening progresses from the equatorward to poleward edges of the pre-existing auroral oval; and a brightening moves sunwards along the length of the TPA1. At 20:23 UT there is a brightening of TPA2 along its whole length, which corresponds to the brightening of TPA2 seen in Fig. 2(b).

We examine this combined brightening of the midnight sector oval and TPA1 in more detail in Figure 4. This figure focusses on the 24 min encompassing the step arrival (vertical green line) and the brightening. Observations are shown from both WIC and SI12, on the left from the noon-midnight meridian, and on the right from a parallel meridian displaced towards dawn so that it runs along the length of TPA1. Two slanted green lines have been added to guide the eye, the same in each panel. The lower line indicates the poleward motion of the brightening of the midnight sector oval, the upper line tracks the brightening sunwards along TPA1: clearly these two effects occur simultaneously.

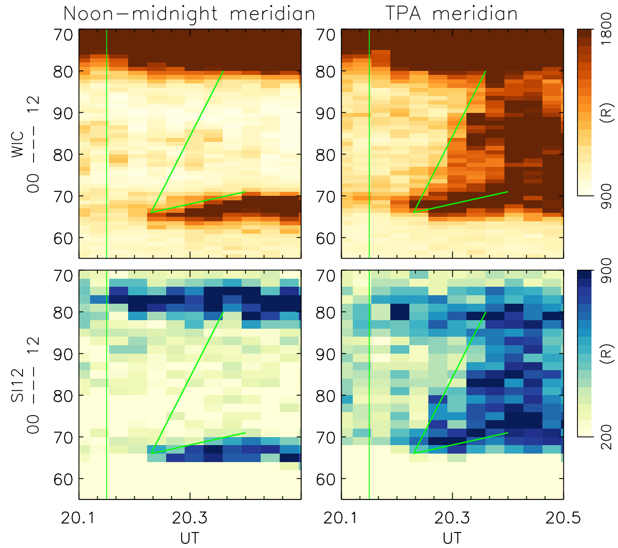

Figure 4. WIC and SI12 keograms encompassing 24 min around the time of the solar wind step arrival (vertical green line), along the noon-midnight meridian and a parallel meridian displaced towards dawn such that it intersects TPA1. Green lines are overlaid to guide the eye.

3 Discussion

We presume that the progression of the brightening of the oval and the TPAs tracks the solar wind step as it engulfs the magnetosphere (Zhou & Tsurutani, 1999; Tsurutani et al., 2001; Meurant et al., 2004; Tsurutani et al., 2011), first impacting the dayside magnetopause, moving around the flanks, and then progressing along the length of the magnetotail. We suggest that as the magnetotail is compressed, a reduction in the radius of curvature of field lines where they cross the neutral sheet causes pitch angle scattering of particles into the loss cone, which in turn produces a brightening of the oval or TPAs. In other words, the TPAs must comprise closed field lines, and as the nightside oval and TPA1 brighten simultaneously they map to similar distances down-tail. As TPA2 brightens last, it maps further down-tail.

The solar wind step is travelling with a speed close to 600 km s^{-1}, meaning that it travels approximately 28 R_E in 5 min. The brightening of the oval from the noon to midnight sectors takes about this time; if the dayside magnetopause is assumed to be located at $X \approx 10\ R_E$, then this suggests that the step has engulfed the magnetosphere to a down-tail position of $X \approx -18\ R_E$, the near-tail plasma sheet, when the midnight sector oval and the nightside end of TPA1 first brighten. The subsequent sunward brightening of the nightside oval and TPA1 take another 10 min, at which point the step has progressed to $X \approx -74\ R_E$ down-tail. This indicates that TPA1 maps to the mid- and far-tail plasma sheet region, the same distances that map to the main oval. TPA2 brightens just after this, so maps to the region $-90 > X > -75\ R_E$.

Figure 5 presents a schematic of our proposed magnetotail structure based upon these observations, at around 20:17 UT when the pressure step has reached the mid-tail. Fig. 5a shows the auroral configuration in the northern hemisphere ionosphere: the white region is the open polar cap, the blue region indicates closed field lines which have brightened at earlier times, the green region is the auroral oval which has yet to brighten, and the orange regions are the closed TPA field lines which also have yet to brighten. We expect the southern hemisphere auroral configuration to be similar to this, but mirrored about $Y = 0$, as suggested by the formation mechanism of Milan et al. (2005). Fig. 5b

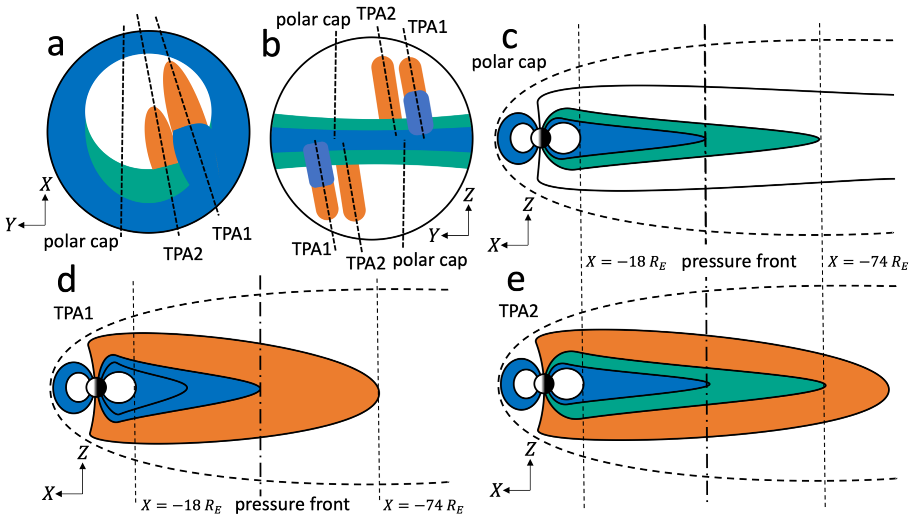

Figure 5. A schematic of the proposed magnetic structure of the magnetosphere, at the time that the solar wind pressure step (dot-dashed line) has reached the mid-tail (around 20:17 UT). (a). The auroral configuration, indicating where the oval and TPA1 has brightened (blue), where the oval has yet to brighten (green), where TPA1 and TPA2 have yet to brighten (orange), and the open polar cap (white). (b) A cross-section of the magnetotail showing closed field lines (coloured) and open field lines (white). (c) The cross-section of the magnetosphere along a meridian cutting through the polar cap, showing field lines where pitch angle scattering has occurred (blue), and where it has yet to occur (green). (d) and (e) Cross-sections of the magnetosphere along meridians intersecting TPA1 and TPA2.

shows a cross-section of the magnetotail near $X = -50\ R_E$; magnetic field lines point into and out of the page in the northern and southern hemispheres, respectively. The white magnetotail lobes connect into the solar wind further down-tail. The TPA field lines are closed and cross the equatorial plane further down-tail. The field lines of the TPAs are contained in limited local time sectors, bisecting the magnetospheric lobes which have their usual structure at earlier and later local times. In this panel we have indicated the proposed location of the TPAs in the southern hemisphere, mirrored about $Y = 0$ as argued above. This suggests that the TPA field lines are not strictly contained within meridional planes, but cross $Y = 0$ further down-tail, such that TPA1 in the northern hemisphere is magnetically connected to TPA1 in the southern hemisphere, and similarly for TPA2. Figs. 5c to e show the mapping of the field lines down-tail; these schematics are not strictly in meridional planes but follow the mapping of TPA1 and TPA2 between the hemispheres. The TPA field-lines are less "tail-like" than the field lines that map to the adjacent main oval and lobes. As the pressure step travels along the magnetotail, the compressed field lines map to progressively higher latitudes and a progressive sunwards brightening is observed in both the main oval and TPA1.

This magnetic field configuration might indicate that there is a reduction in the cross-tail current in the locality of the TPAs, as the field is less tail-like where they cross $Z = 0$, and this could lead to a field-aligned current structure reminiscent of a narrow substorm current wedge (see, e.g., Kepko et al. (2015)). Moreover, the field lines that comprise the TPAs are clearly distinct from the field lines comprising the adjacent dawn-side oval, and hence the TPAs do not represent a poleward extension of the plasma sheet in this local time sector.

TPA2 brightens last, indicating that its field lines stretch slightly further down-tail that the field lines comprising the main oval plasma sheet and TPA1. As TPA2 formed after TPA1, this suggests that the magnetic reconnection that closed these field lines occurred in the distant tail near $X \approx -75R_E$, rather than at a near-Earth neutral line, which is supposed to occur in the region $-30 > X > -20\ R_E$. This places a constraint on the location of tail reconnection occurring under northward IMF conditions.

4 Conclusions

The progressive brightening of the auroral oval and a pair of transpolar arcs (TPA1 and TPA2) in response to the compression of the magnetosphere by a solar wind pressure step has allowed us for the first time to remotely-sense the magnetic structure of TPAs. The oval brightened first at noon, then around the flanks (electron and proton auroras dominated at dawn and dusk, respectively), then onto the low-latitude portion of the nightside oval. The nightside oval then brightened polewards, simultaneously with a sunward brightening of TPA1. TPA2 brightened last of all. We conclude that the TPAs comprised closed field lines in a narrow local time sector that map to the plasma sheet between (approximately) $-90 > X > -18\ R_E$. The poleward edge of the midnight-sector main oval and the sunward tip of TPA1 brightened at the same time, indicating that they mapped to similar distances down-tail. TPA2, which formed more recently than TPA1, brightened last, suggesting that its field lines mapped even further down-tail. As the two TPAs appeared adjacent to each other in the polar cap, the magnetic mapping from the ionosphere to the distant magnetotail was complex. The inferred mapping of TPA1 suggests that the edges of the TPA may be associated with field-aligned currents which could arise due to a reduction of the cross-tail current in the local time sector of the TPAs.

The region to which the TPAs mapped are rarely accessed by spacecraft. This unique set of observations has allowed us to probe the complex magnetic structure of the distant magnetotail under northward IMF conditions.

Acknowledgments

SEM and JAC are supported by the Science and Technology Facilities Council (STFC), UK, grant no. ST/N000749/1. BH is supported by the Belgian National Fund for Scientific Research (FNRS). We acknowledge use of NASA/GSFC's Space Physics Data Facility's CDAWeb service (at http://cdaweb.gsfc.nasa.gov), and OMNI data. The OMNI data, including solar wind parameters and geomagnetic indices, and the IMAGE WIC and SI12 data were obtained from CDAWeb.

References

Carlson, H., & Cowley, S. (2005). Accelerated polar rain electrons as the source of sun-aligned arcs in the polar cap during northward interplanetary magnetic field conditions. *Journal of Geophysical Research: Space Physics*, *110*(A5).

Carter, J. A., Milan, S. E., Fear, R., Walach, M.-T., Harrison, Z., Paxton, L., & Hubert, B. (2017). Transpolar arcs observed simultaneously in both hemispheres. *Journal of Geophysical Research: Space Physics*, *122*(6), 6107–6120.

Chisham, G., Lester, M., Milan, S. E., Freeman, M., Bristow, W., Grocott, A., ... others (2007). A decade of the Super Dual Auroral Radar Network (SuperDARN): Scientific achievements, new techniques and future directions. *Surveys in geophysics*, *28*(1), 33–109.

Cowley, S., & Lockwood, M. (1992). Excitation and decay of solar wind-driven flows in the magnetosphere-ionosphere system. In *Annales geophysicae* (Vol. 10, pp. 103–115).

Fear, R. (2019). The northward imf magnetosphere. *AGU Centennial monograph*, *in press*.

Fear, R., & Milan, S. (2012a). The IMF dependence of the local time of transpolar arcs: Implications for formation mechanism. *Journal of Geophysical Research: Space Physics*, *117*(A3).

Fear, R., & Milan, S. (2012b). Ionospheric flows relating to transpolar arc formation. *Journal of Geophysical Research: Space Physics*, *117*(A9).

Fear, R., Milan, S., Maggiolo, R., Fazakerley, A., Dandouras, I., & Mende, S. (2014). Direct observation of closed magnetic flux trapped in the high-latitude magnetosphere. *Science*, *346*(6216), 1506–1510.

Goudarzi, A., Lester, M., Milan, S., & Frey, H. (2008). Multi-instrumentation observations of a transpolar arc in the northern hemisphere. *Annales Geophysicae*, *26*(1), 201–210.

Hosokawa, K., Kullen, A., Milan, S., Reidy, J., Zou, Y., Frey, H., ... Fear, R. (2019). Aurora in the polar cap: a review. *Space Science Reviews*, *in press*.

Kepko, L., McPherron, R., Amm, O., Apatenkov, S., Baumjohann, W., Birn, J., ... Sergeev, V. (2015). Substorm current wedge revisited. *Space Science Reviews*, *190*(1-4), 1–46.

King, J., & Papitashvili, N. (2005). Solar wind spatial scales in and comparisons of hourly Wind and ACE plasma and magnetic field data. *Journal of Geophysical Research: Space Physics*, *110*(A2).

Kullen, A. (2012). Transpolar arcs: Summary and recent results. *Auroral Phenomenology and Magnetospheric Processes: Earth and Other Planets, Geophys. Monogr. Ser*, *197*, 69–80.

Kullen, A., Fear, R., Milan, S. E., Carter, J., & Karlsson, T. (2015). The statistical difference between bending arcs and regular polar arcs. *Journal of Geophysical Research: Space Physics*, *120*(12), 10–443.

Mailyan, B., Shi, Q., Kullen, A., Maggiolo, R., Zhang, Y., Fear, R., ... others (2015). Transpolar arc observation after solar wind entry into the high-latitude magnetosphere. *Journal of Geophysical Research: Space Physics*, *120*(5), 3525–3534.

Mende, S., Heetderks, H., Frey, H., Lampton, M., Geller, S., Abiad, R., ... others (2000). Far ultraviolet imaging from the IMAGE spacecraft. 2. Wideband FUV imaging. In *The IMAGE Mission* (pp. 271–285). Springer.

Mende, S., Heetderks, H., Frey, H., Lampton, M., Geller, S., Habraken, S., ... others (2000). Far ultraviolet imaging from the IMAGE spacecraft. 1. System design. *Space Science Reviews*, *91*(1-2), 243–270.

Mende, S., Heetderks, H., Frey, H., Stock, J., Lampton, M., Geller, S., ... others (2000). Far ultraviolet imaging from the image spacecraft. 3. spectral imaging of Lyman-α and OI 135.6 nm. In *The IMAGE Mission* (pp. 287–318). Springer.

Meurant, M., Gérard, J.-C., Blockx, C., Hubert, B., & Coumans, V. (2004). Propagation of electron and proton shock-induced aurora and the role of the interplanetary magnetic field and solar wind. *Journal of Geophysical Research: Space Physics*, *109*(A10).

Meurant, M., Gérard, J.-C., Hubert, B., Coumans, V., Blockx, C., Østgaard, N., & Mende, S. (2003). Dynamics of global scale electron and proton precipitation induced by a solar wind pressure pulse. *Geophysical research letters*, *30*(20).

Milan, S. E., Hubert, B., & Grocott, A. (2005). Formation and motion of a transpolar arc in response to dayside and nightside reconnection. *Journal of Geophysical Research: Space Physics*, *110*(A1).

Milan, S. E., Lester, M., Cowley, S., Oksavik, K., Brittnacher, M., Greenwald, R., ... Villain, J.-P. (2003). Variations in the polar cap area during two substorm cycles. *Annales Geophysicae*, *21*(5), 1121–1140.

Milan, S. E., Provan, G., & Hubert, B. (2007). Magnetic flux transport in the dungey cycle: A survey of dayside and nightside reconnection rates. *Journal of Geophysical Research: Space Physics*, *112*(A1).

Newell, P. T., Liou, K., & Wilson, G. R. (2009). Polar cap particle precipitation and aurora: Review and commentary. *Journal of Atmospheric and Solar-Terrestrial Physics*, *71*(2), 199–215.

Østgaard, N., Mende, S., Frey, H., Frank, L., & Sigwarth, J. (2003). Observations of non-conjugate theta aurora. *Geophysical Research Letters*, *30*(21).

Reidy, J. A., Fear, R., Whiter, D., Lanchester, B., Kavanagh, A. J., Milan, S., … Zhang, Y. (2018). Interhemispheric survey of polar cap aurora. *Journal of Geophysical Research: Space Physics*, *123*(9), 7283–7306.

Shi, Q., Zong, Q.-G., Fu, S., Dunlop, M., Pu, Z., Parks, G., … others (2013). Solar wind entry into the high-latitude terrestrial magnetosphere during geomagnetically quiet times. *Nature communications*, *4*, 1466.

Tsurutani, B., Lakhina, G., Verkhoglyadova, O. P., Gonzalez, W., Echer, E., & Guarnieri, F. (2011). A review of interplanetary discontinuities and their geomagnetic effects. *Journal of Atmospheric and Solar-Terrestrial Physics*, *73*(1), 5–19.

Tsurutani, B., Zhou, X.-Y., Arballo, J., Gonzalez, W., Lakhina, G., Vasyliunas, V., … others (2001). Auroral zone dayside precipitation during magnetic storm initial phases. *Journal of Atmospheric and Solar-Terrestrial Physics*, *63*(5), 513–522.

Zhou, X., & Tsurutani, B. T. (1999). Rapid intensification and propagation of the dayside aurora: Large scale interplanetary pressure pulses (fast shocks). *Geophysical Research Letters*, *26*(8), 1097–1100.

Zhu, L., Schunk, R., & Sojka, J. (1997). Polar cap arcs: a review. *Journal of Atmospheric and Solar-Terrestrial Physics*, *59*(10), 1087 - 1126. doi: https://doi.org/10.1016/S1364-6826(96)00113-7

Figure 1.

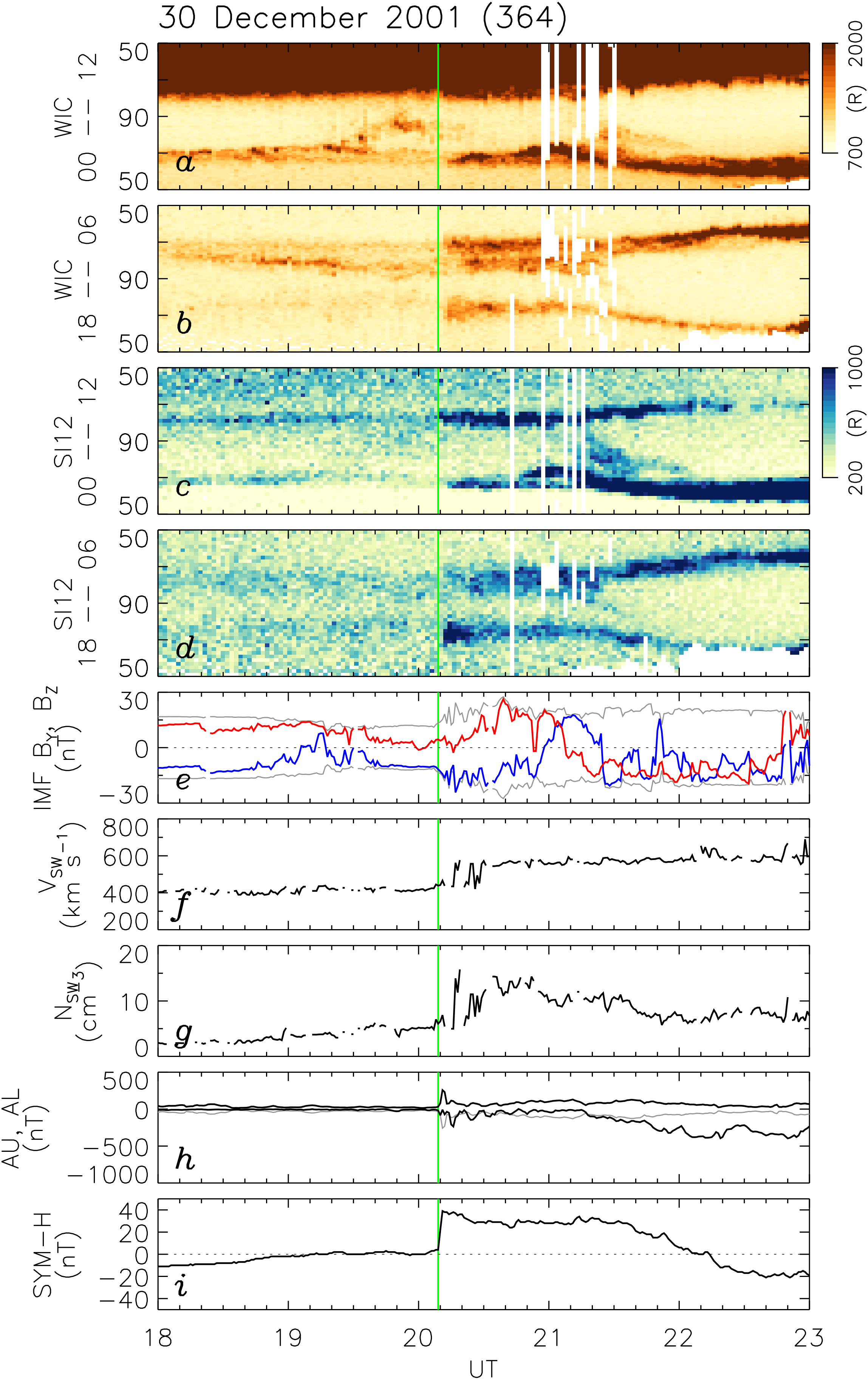
30 December 2001 (364)
WIC 00 -- 12
WIC 18 -- 06
SI12 00 -- 12
SI12 18 -- 06
50
90
50
2000
(R)
700
1000
(R)
200
a
b
c
d
e
f
g
h
i
IMF By, Bz (nT)
30
0
−30
Vsw (km s−1)
800
600
400
200
Nsw (cm−3)
20
10
0
AU, AL (nT)
500
0
−500
−1000
SYM−H (nT)
40
20
0
−20
−40
18
19
20
21
22
23
UT

Figure 2.

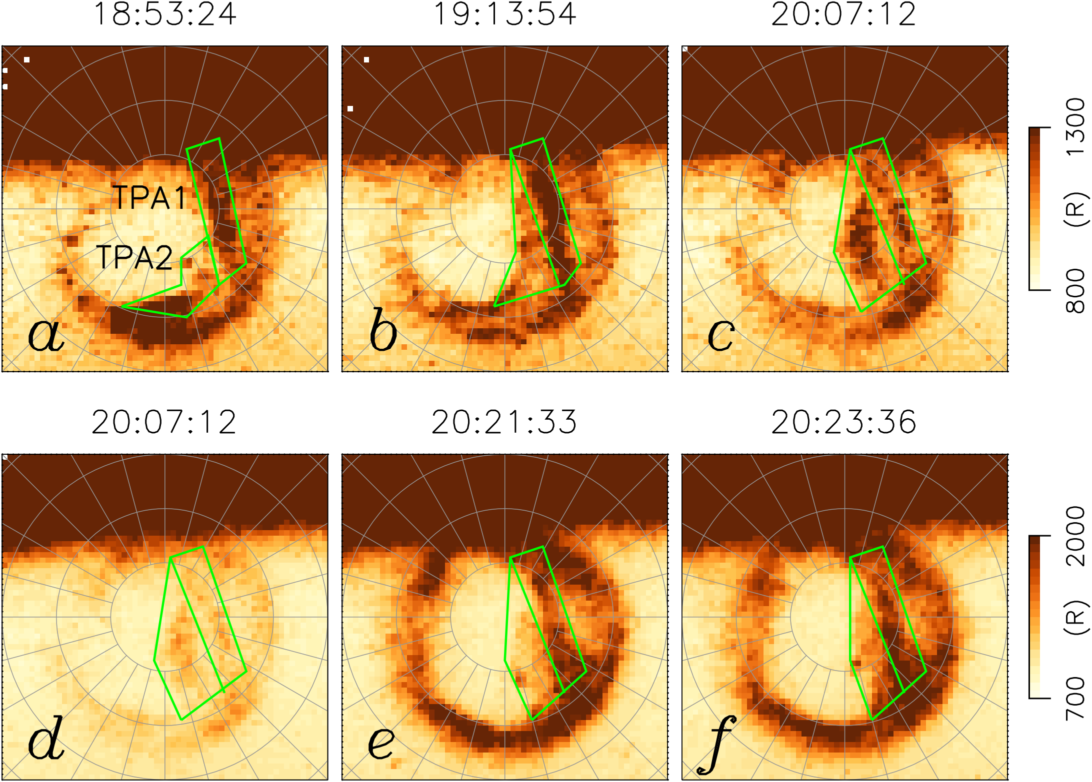
18:53:24
19:13:54
20:07:12
TPA1
TPA2
a
b
c
1300
(R)
800
20:07:12
20:21:33
20:23:36
d
e
f
2000
(R)
700

Figure 3.

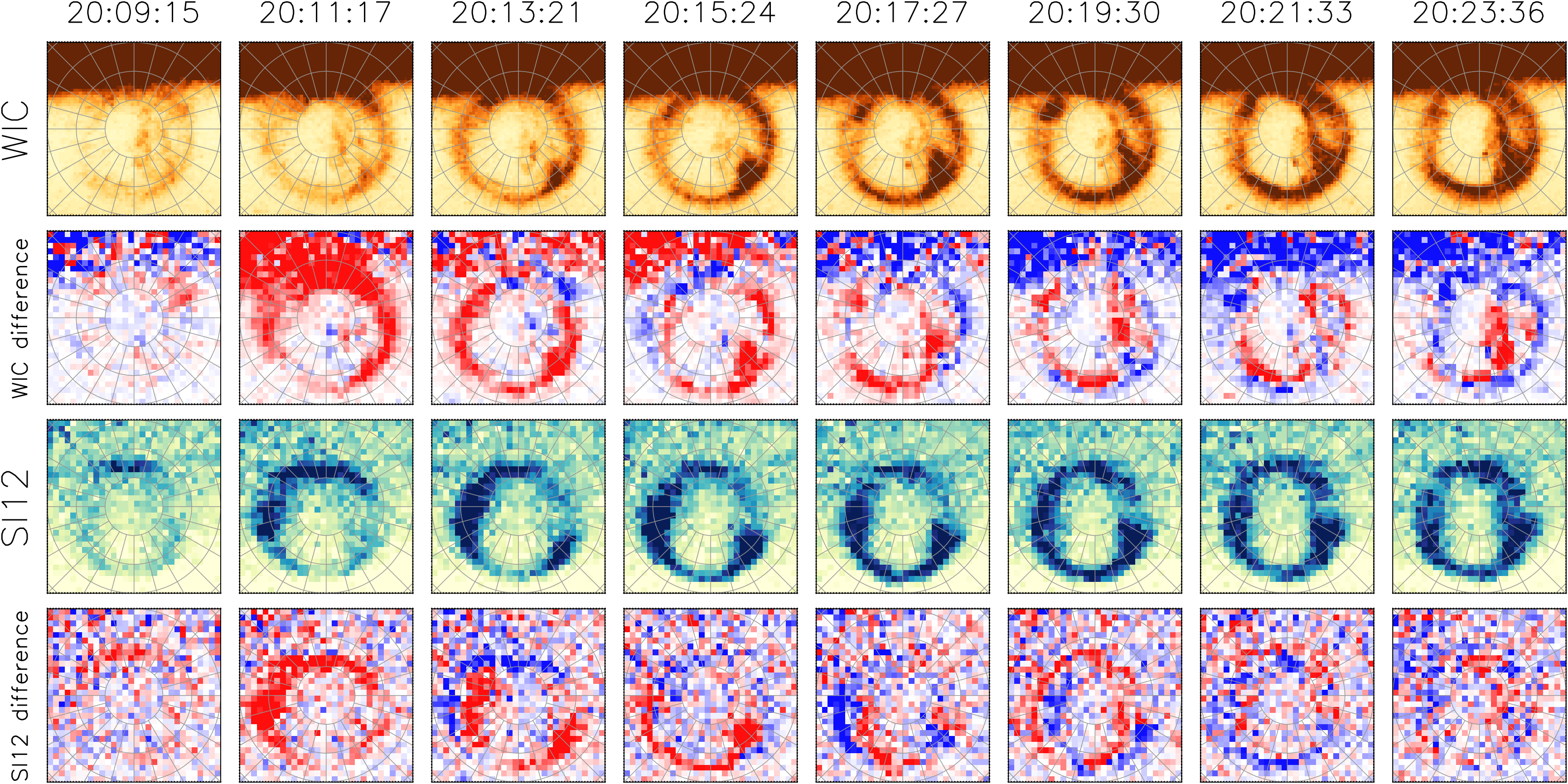
20:09:15
20:11:17
20:13:21
20:15:24
20:17:27
20:19:30
20:21:33
20:23:36
WIC
WIC difference
SI12
SI12 difference

Figure 4.

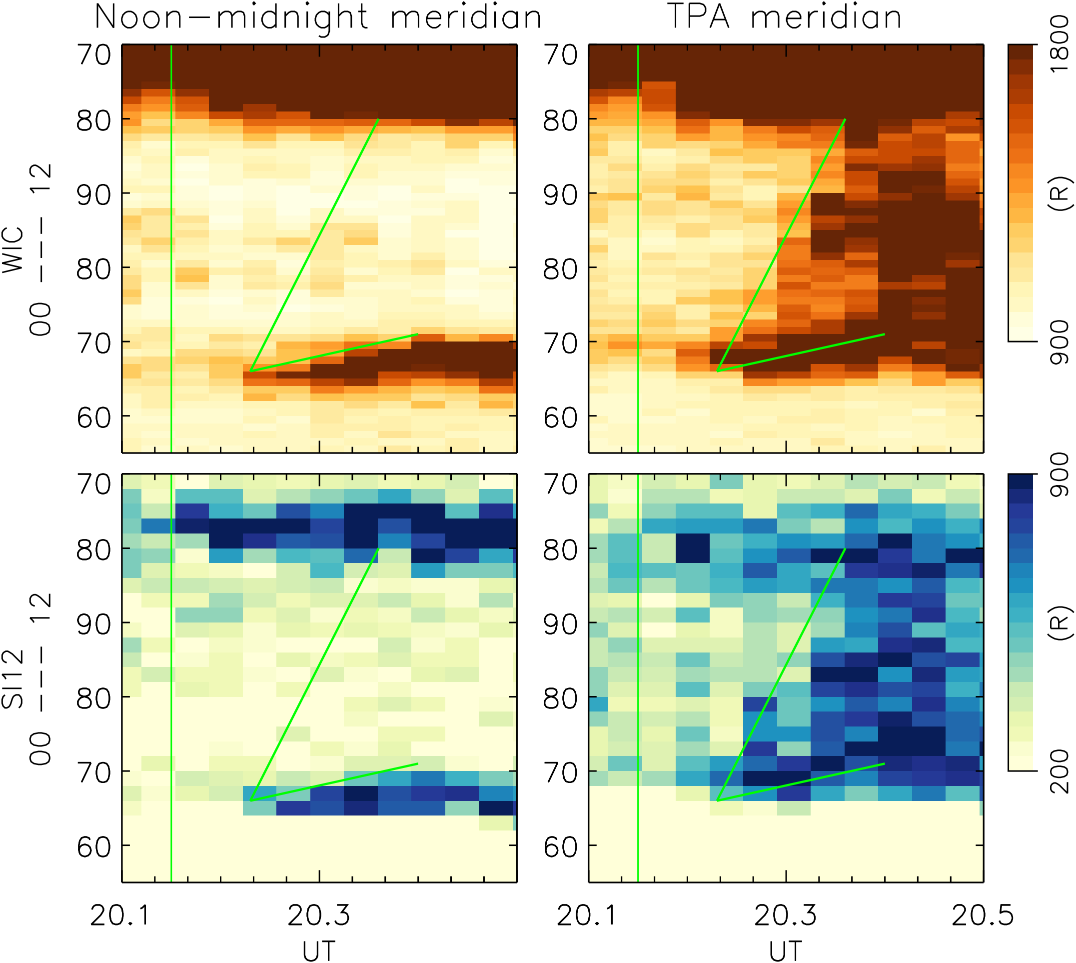
Noon−midnight meridian
TPA meridian
WIC
00 --- 12
SI12
00 --- 12
70
80
90
80
70
60
1800
(R)
900
200
20.1
20.3
20.5
UT

Figure 5.

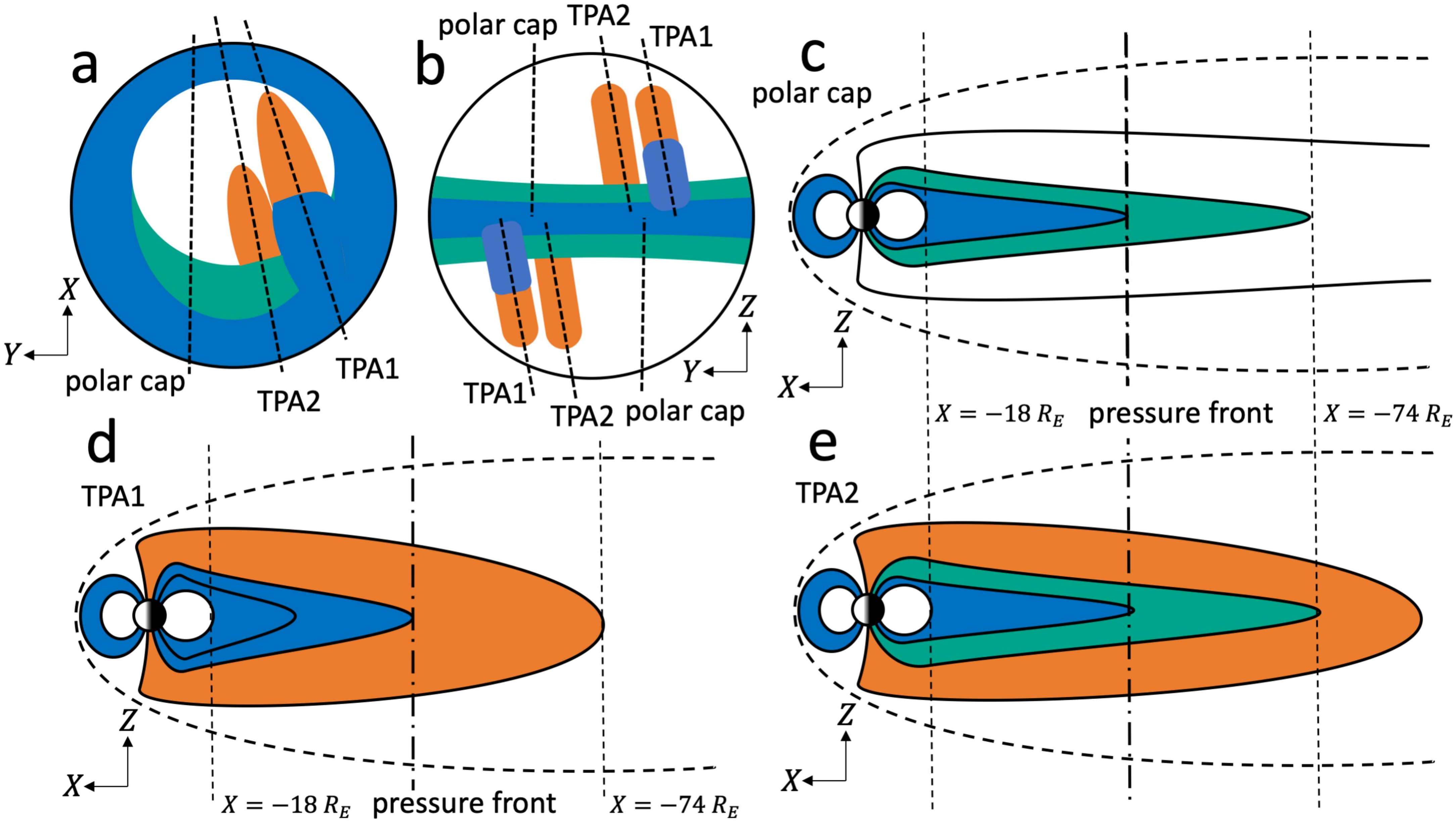
a
polar cap
TPA2
TPA1
X
Y
b
polar cap
TPA2
TPA1
TPA1
TPA2
polar cap
Z
Y
c
polar cap
Z
X
$X = -18\ R_E$
pressure front
$X = -74\ R_E$
d
TPA1
Z
X
$X = -18\ R_E$
pressure front
$X = -74\ R_E$
e
TPA2
Z
X